Optimal Receiver Bandwidth for Energy-Detection PPM UWB Systems

Jose M. Almodovar-Faria and Janise McNair
Electrical and Computer Engineering
University of Florida
Gainesville, FL

David Wentzloff
Electrical Engineering and Computer Science
University of Michigan
Ann Arbor, MI

***Abstract*—Non-coherent UWB receivers are often implemented using energy detection architectures which are very sensitive to noise in the channel and interference. Therefore, the receiver bandwidth plays an important role since the total noise and interference energy is proportional to this bandwidth. This work provides analytical expressions to find the optimal receiver bandwidth and quantifying the effect on the bit-error-rate (BER) due to channel noise and adjacent-channel interference (ACI). A reduction in receiver bandwidth beyond the optimal point is shown to have minimal impact on BER performance when ACI is negligible.**

Keywords- ultra-wideband; non-coherent; energy detection; pulse-position modulation; bandwidth; bit-error-rate; adjacent-channel interference; signal-to-noise ratio per bit

I. INTRODUCTION

Pulse-based digital communications, such as pulse position modulation (PPM), are commonly used to implement low power UWB impulse radios. These radios can be realized using coherent or non-coherent architectures. For instance, in terms of data rate and bit-error-rate (BER), coherent receivers perform better than non-coherent [1][2]. However, non-coherent receivers offer simpler architecture and lower power compared to coherent receivers [1]. Therefore, non-coherent architectures are attractive solutions for low cost, low complexity, and very low power applications [3-6].

Non-coherent receivers are typically implemented using architectures based on energy detection (ED) [7-12]. Figure 1 shows the generic ED architecture. As shown, after channel selection and amplification, the transmitted signal is squared and integrated in order to measure its energy. Bit slicing is then carried out by comparing energies in two time windows or integration windows. Due to this principle of energy comparison, ED receivers are very sensitive to noise in the channel (i.e. an increase in noise energy increases the probability of bit-error). Assuming an additive white Gaussian noise (AWGN) channel, the noise energy varies proportionally to the size of the integration window and the filter bandwidth due to its flat power spectrum. Hence, the band-pass filter (BPF) as well as the integration window plays an important role in the receiver performance.

According to the amendment of IEEE P802.15.4a [13], at the maximum radiation frequency, the 10dB-bandwidth of an UWB signal must be at least 500MHz. Based on this definition, it is common to design UWB systems where the bandwidths for receiver and transmitter circuits are chosen to be equal to the 10dB-bandwidth of the transmitted signal [2][6-8][14]. However, using a receiver bandwidth that is smaller than the pulsed signal bandwidth (i.e. using a BPF with pass-band smaller than the signal bandwidth) relaxes the specifications on the receiver circuits (e.g. LNA bandwidth, ADC sample rate) while reducing the integration of noise energy.

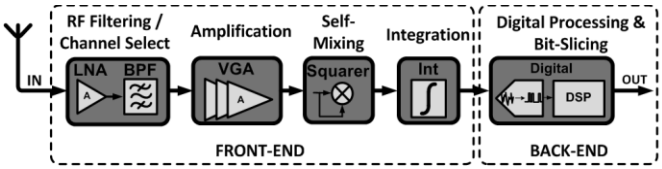

Fig 1. Non-coherent ED Receiver Architecture

There is related-work regarding optimal bandwidth for ED receivers. In [17], the well-known BER equation for a 2-PPM ED receiver is used in two cases of study to graphically show that there exists an optimal receiver bandwidth for different input signal-to-noise ratio (SNR). In this work, we derive a general equation that is independent of SNR and from which the optimal receiver bandwidth can be calculated as a function of the signal's 10dB-bandwidth, the integration time, and the desired BER. In addition, the effect of adjacent-channel interference (ACI) is included in the analysis.

II. BACKGROUND

This section is divided in two parts. The first part shows the BER expression for energy-detection (ED) receivers using PPM modulation. The second part focuses on the effect of BPF bandwidth reduction.

A. Probability of Bit-Error

The probability of bit-error for a non-coherent PPM receiver based on energy detection and sampled at the Nyquist frequency is given by [15] [18]

$$BER \approx Q\left(\frac{E_b/N_o}{\sqrt{2 \cdot T_i \cdot \Delta f \; + \; 2 \cdot E_b/N_o}}\right) \qquad (1)$$

where $Q(x)$ is the Q-function, E_b is the energy per bit, N_o is the noise spectral density, T_i is the time of integration, and Δf is the receiver bandwidth. Equation (1) is derived using the central-limit theorem to approximate the random variables that represent the squared signal as Gaussian random variables. In order for this approximation to be valid $T_i \cdot \Delta f \geq 20$ [18].

B. Effect of Receiver Bandwidth Reduction

In the introduction we motivated the importance of the BPF based on the fact that ED architectures are very sensitive to noise in the channel. Thus, the impact of noise on BER performance can be reduced by maximizing the signal-to-noise ratio (SNR). This can be inferred from (1) since $E_b/N_o \propto SNR$. By carefully choosing the BPF bandwidth, we can maximize the SNR which is given now by

$$SNR = \frac{P_s - \Delta P_s}{P_n - \Delta P_n} = \frac{P_s}{P_n}\left(\frac{1 - \Delta P_s/P_s}{1 - \Delta P_n/P_n}\right) \quad (2)$$

where, as shown in figure 2, ΔP_s and ΔP_n are the reduction in signal and noise powers, respectively, and P_s and P_n are the nominal signal and noise powers when the receiver bandwidth is equal to the 10dB-bandwidth of the transmitted signal.

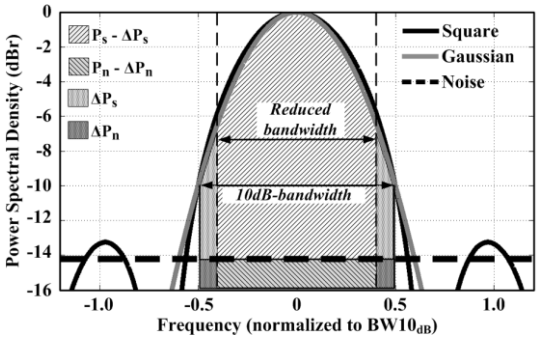

Fig 2. Power spectral densities of a square pulse, Gaussian pulse, and AWGN

As BPF bandwidth is decreased from the 10dB-bandwidth, the numerator of (2) decreases at a slower rate than the denominator (i.e. $\Delta P_s/P_s < \Delta P_n/P_n$). Hence, SNR increases until $\Delta P_s/P_s$ is no longer smaller than $\Delta P_n/P_n$. The maximum value for SNR is achieved when the rate of change of $\Delta P_s/P_s$ and $\Delta P_n/P_n$ is equal. This can be graphically seen in figure 3. Both signal and noise power increase as frequency increases; however, $\Delta P_s/P_s < \Delta P_n/P_n$ remains true until the slope (i.e. rate of change) of the signal power is equal to the slope of the noise energy (i.e. $\Delta P_s/P_s = \Delta P_n/P_n$). At this point, SNR is maximized.

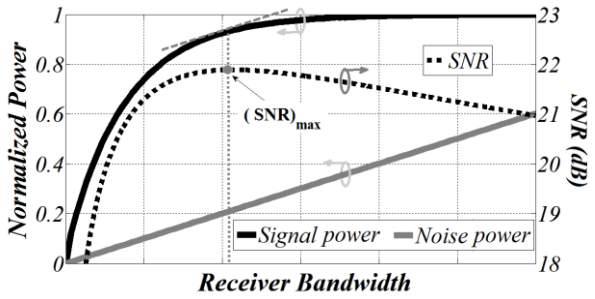

Fig 3. Signal and noise power profile.

III. Modified Probability of Bit-Error and Optimal Receiver Bandwidth

In this section, (1) is modified to include the effect of reducing the BPF bandwidth. For convenience and comparison purposes, the receiver bandwidth is normalized to the commonly used 10dB-bandwidth (i.e. $\beta = \Delta f/B$ where Δf is the BPF bandwidth and B is the 10dB-bandwidth of the signal). Furthermore, square pulses are used as the transmitted signal because they are commonly used due to the simplicity to generate them. Nevertheless, the results are similar for other pulse shapes such as Gaussian since the power spectral density (PSD) of a Gaussian pulse is comparable to that of a square pulse inside the 10dB-bandwidth (less than 3% of power difference) as shown in figure 2.

A. Probability of Bit-Error and Receiver Bandwidth

The Fourier transform of a square pulse with time width T_P is given by the sinc function

$$V_{T_p}(f) = T_P \frac{\sin(\pi T_P f)}{\pi T_P f} \quad (3)$$

Recall that the energy spectral density (ESD) is given by $S_E(f) = |V_{T_P}(f)|^2$. Then, integrating $S_E(f)$ over a range of frequencies gives the total energy of the signal over that range. Thus, the pulse energy for a filter bandwidth Δf is

$$E_b(\Delta f) = \int_{-\frac{\Delta f}{2}}^{\frac{\Delta f}{2}} S_E(f)\, df = 2\int_0^{\frac{\Delta f}{2}} \left| T_P \frac{\sin(\pi T_P f)}{(\pi T_P f)} \right|^2 df \quad (4)$$

$$E_b(\Delta f) = \frac{2 \cdot [\cos(\pi T_P \Delta f) + \pi T_P \Delta f \cdot Si(\pi T_P \Delta f) - 1]}{\pi^2 \Delta f} \quad (5)$$

where $Si(x) = \int_0^x sin(t)/t\ dt$.

As mentioned before, the receiver bandwidth is normalized to the signal bandwidth (i.e. $\beta = \Delta f/B$), which can be derived using the Taylor series of a sinc function and can be accurately approximated by $B \approx 1.476/T_P$. Hence, (5) becomes

$$E_b(\beta) = \frac{2[\cos(1.476\pi\beta) + 1.476\pi\beta Si(1.476\pi\beta) - 1]}{\pi^2 \cdot \beta \cdot B} \quad (6)$$

Reducing the receiver bandwidth decreases the signal energy E_b as explained in section II.B (see figure 3). Therefore, a bandwidth reduction results in a decreased SNR-per-bit (i.e. E_b/N_o) since the noise spectral density is constant. Thus, an SNR-per-bit scaling factor $\delta(\beta)$ can be obtained by normalizing (6) to the signal energy of the full 10dB-bandwidth, i.e. $E_b(\beta = 1)$. Thus, the scaling factor is given by

$$\delta(\beta) = \frac{E_b(\beta)}{E_b(\beta = 1)} \quad (7)$$

Incorporating $\delta(\beta)$ into (1) and substituting $\Delta f = \beta \cdot B$ gives an expression for BER that depends on the normalized bandwidth β. Then, (1) can be rewritten as

$$BER(\beta) = Q\left(\frac{\delta(\beta) \cdot (E_b/N_o)}{\sqrt{2 \cdot T_i \cdot \beta \cdot B + 2 \cdot \delta(\beta) \cdot (E_b/N_o)}}\right) \quad (8)$$

This expression predicts the BER of a receiver as a function of the normalized bandwidth $\beta = \Delta f/B$ for a specific value of E_b/N_o. However, we are often more interested in the required E_b/N_o to meet a target BER; therefore, solving (8) for E_b/N_o gives the required SNR-per-bit

$$SNR_{bit}(\beta) = \left(\frac{E_b}{N_o}\right) = \frac{K^2}{\delta(\beta)}\left(1 + \sqrt{1 + \frac{2 \cdot T_i \cdot B \cdot \beta}{K^2}}\right) \quad (9)$$

where T_i is the integration time and $K = Q^{-1}(BER)$. Equation (9) can be used to obtain an optimal bandwidth as will be shown next.

B. Optimal Receiver Bandwidth

The optimal receiver bandwidth is the value that minimizes $SNR_{bit}(\beta)$. To find this optimal value, a local minimum must be found for (9). Thus, the optimal values are given by

$$\beta_{opt} = Solve\left\{\frac{\partial}{\partial\beta}[SNR_{bit}(\beta)] = 0, \beta\right\} \quad (10)$$

Equation (10) cannot be solved explicitly mainly due to the complexity of the scaling factors $\delta(\beta)$. Thus, to obtain a solution for β_{opt}, approximations for $\sqrt{1 + (2T_iB/K^2)\cdot\beta}$ and $\delta(\beta)$ are used. For mathematical simplicity, a non-linear least-square regression is used with the exponential fit

$$y_i = a_i + b_i \cdot \exp(c_i + d_i \cdot x) \quad (11)$$

where x is the regression parameter (i.e. the independent variable), a_i, b_i, c_i, d_i are constants, and $i = 1, 2$ identifies the desired approximation ($i = 1$ for $\sqrt{1+X}$ and $i = 2$ for $\delta(\beta)$). The values for the constants are shown in table I. Now, using (11) to estimate (9) gives this approximation

$$SNR_{bit}(\beta) \approx K^2 \cdot \frac{1 + a_1 + b_1 exp(c_1 + d_1 \cdot N \cdot \beta)}{a_2 + b_2 exp(c_2 + d_2 \cdot \beta)} \quad (12)$$

where $N = 2 \cdot T_w \cdot B/K^2$. Equation (12) can be used to solve (10). Taking its derivative and then solving for β gives the optimal normalized bandwidth β_{opt} which can be approximated by

$$\beta_{opt} \approx A_\beta + \frac{\ln(B_\beta/N)}{C_\beta + N \cdot D_\beta} \quad (13)$$

The constants in (13) are summarized in table II for 3 different ranges of N and a maximum error of less than 1%.

TABLE I. CONSTANT VALUES FOR EQUATION (11)

i	Parameter	Regression parameter	a_i	b_i	c_i	d_i
1	$\sqrt{1+X}$	$1 \le X < 10$	4.82	-0.66	1.73	-0.089
		$10 \le X < 50$	10.78	-1.35	1.89	-0.018
		$50 \le X < 250$	22.9	-11.77	0.49	-0.004
2	$\delta(\beta)$	$0.3 \le \beta < 1$	1.138	-0.10	2.60	-2.35

TABLE II. CONSTANT VALUES FOR EQUATION (13)

Range	A_β	B_β	C_β	D_β
$1 \le N < 10$	0.775	67.5	17.1	1.355
$10 \le N < 50$	0.766	50.0	19.5	0.350
$50 \le N < 250$	0.742	120.0	33.0	0.100

IV. ADJACENT-CHANNEL INTERFERENCE

The analysis in this section assumes square pulses as the interference signal. The idea behind this analysis is to gain a better understanding on how the filter bandwidth changes the BER performance of a PPM receiver in the presence of other transmitters with similar signals in different channels.

A. Effect of Adjacent-Channel Interference on the Receiver Performance

In the last years, several papers related to UWB interference have been published and among them are [19]-[23]. Different approaches to model in-band UWB interference can be found in literature. However, many of them agree in a Gaussian approximation model [21]-[23]. Consequently, here adjacent-channel interference (ACI) is treated as AWGN and modeled with a flat power spectrum.

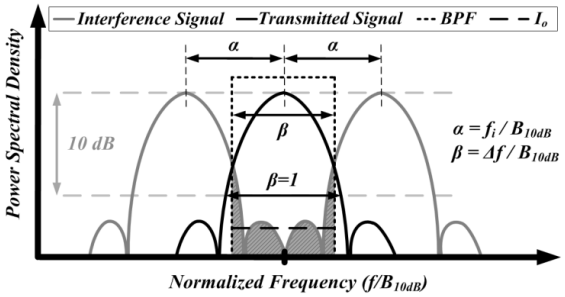

Fig 4. Frequency spectrum of the transmitted signal with ACI

Figure 4 shows the spectrum of the signal with adjacent-channel interference, the BPF impulse response, and the interference spectral density I_o. The shaded region represents the interference energy. To calculate this energy, (6) can be used with different integration limits. Then,

$$E_i(f_i, \Delta f) = \int_{f_i - \frac{\Delta f}{2}}^{f_i + \frac{\Delta f}{2}} \left| T_P \frac{\sin(\pi T_P f)}{(\pi T_P f)} \right|^2 df \quad (14)$$

where f_i is the frequency space between the transmitted and the interference signal (i.e. channel spacing) and Δf is the BPF bandwidth (see figure 4). Again, for convenience, f_i and Δf are normalized to the 10dB-bandwidth of the signal (i.e. $\alpha = f_i/B$, $\beta = \Delta f/B$). Then, by solving (14), the ACI energy can be expressed as

$$E_i(\alpha, \beta) = \frac{\left[\frac{cos(c\rho_1)}{\rho_1} + \frac{cos(c\rho_2)}{\rho_2} + c[Si(c\rho_2) + Si(c\rho_1)] - \frac{2\beta}{\rho_1\rho_2}\right]}{\pi^2 B} \quad (15)$$

where $c = 1.476\pi$, $\rho_1 = (\beta - 2\alpha)$, and $\rho_2 = (\beta + 2\alpha)$. Now, recall the assumption of flat power spectrum for ACI. Then, the interference spectral density is given by $I_o = P_i/\Delta f$, where P_i is the interference average power. The interference average power due to a single 1-sided adjacent interferer can be approximated by $P_i = E_i'(\alpha, \beta)/(2 \cdot T_w)$. Therefore, the spectral density of multiple 2-sided adjacent interferers is

$$I_o(\alpha, \beta) = \frac{2}{T_i \cdot \beta \cdot B} \sum_{k=1}^{m} \frac{E_i(k \cdot \alpha, \beta)}{\varepsilon_k} \quad (16)$$

where m is the total number of 2-sided interferers in the channel (e.g. $m = 1$ in figure 4) and $\varepsilon_k = E_b(1)/E_i(0,1)$ is the signal-to-interference ratio (SIR) of the k^{th} 2-sided interferer,

i.e. the received-power ratio of the transmitted signal and the k^{th} 2-sided interference signal (e.g. $\varepsilon_k = 1 \ \forall\, 0 < k < m$ if all transmitters in a wireless network are at the same distance from the receiver and they all use the same transmission power).

To account for ACI, an effective SNR-per-bit, $(E_b/N_o)_{eff}$, can be used in (1). Since the interference is modeled by a Gaussian approximation as motivated earlier, the effective SNR-per-bit can be expressed as $(E_b/N_o)_{eff} = E_b/(N_o + I_o)$ which is often called the signal-to-interference-and-noise ratio (SINR). Here, $N_o = E_b/(E_b/N_o)$, $I_o = I_o(\alpha, \beta)$, and $E_b \approx E_b(\beta = 1)$. Thus,

$$\left(\frac{E_b}{N_o}\right)_{eff} = \left[\frac{1}{(E_b/N_o)} + \frac{I_o(\alpha,\beta)}{E_b(1)}\right]^{-1} \tag{17}$$

By substituting E_b/N_o for $(E_b/N_o)_{eff}$ in the equations derived in section II.A, the effect of ACI can be taken into account. Hence, (8) can be written as

$$BER(\alpha,\beta) = Q\left(\frac{(E_b/N_o)_{eff}}{\sqrt{2 \cdot T_w \cdot \beta \cdot B \ + \ 2 \cdot (E_b/N_o)_{eff}}}\right) \tag{18}$$

Solving (18) for E_b/N_o gives the required SNR-per-bit as a function of the receiver bandwidth (β)

$$SNR_{bit}(\alpha,\beta) = \left[\frac{\delta(\beta)}{K^2 \cdot \left(1 + \sqrt{1 + \frac{2 \cdot T_i \cdot B \cdot \beta}{K^2}}\right)} - \frac{1}{SIR_{bit}(\alpha,\beta)}\right]^{-1} \tag{19}$$

where $SIR_{bit}(\alpha,\beta) = E_b(1)/I_o(\alpha,\beta)$.

B. An Approximation for the Optimal Receiver Bandwidth

Equation (19) can only be solved numerically due to its complexity. However, by following the approach on section IV and making some assumptions, an expression for β_{opt} can be obtained. In this case, let's assume the following:

1) Only the first 2-sided ACI is significant (i.e. $m = 1$) and it has a unitary SIR (i.e. $\varepsilon_1 = 1$).

2) Using the exponential fit used in section IV, $E_i(\alpha,\beta) \approx 0.5 \cdot [exp(3.35 + 3.85 \cdot \rho_1) - exp(-3.35 + 3.85 \cdot \rho_2)]$.

3) The ACI signal has the same bandwidth as the transmitted signal.

For these assumptions, the optimal bandwidth can be calculated by solving (10) using the expression for $SNR_{bit}(\alpha,\beta)$ given in (19). This yields the following approximation

$$\beta_{opt} \approx A_\beta + \frac{\ln(B_\beta/N) - (E_\beta/\alpha) \cdot \ln(F_\beta/\alpha)}{C_\beta + N \cdot D_\beta} \tag{20}$$

where A_β, B_β, C_β, D_β are given in table II, $E_\beta = 5.20$, $F_\beta = 0.89$ and $10 \le N < 50$. Recall that $N = 2 \cdot T_i \cdot B/K^2$.

V. Simulation Setup

To support and corroborate the theory developed, a simulator for a non-coherent PPM receiver based on energy detection was built in MATLAB. Figure 5 shows the overall simulator diagram. It has three major parts: modulation, channel modeling, demodulation.

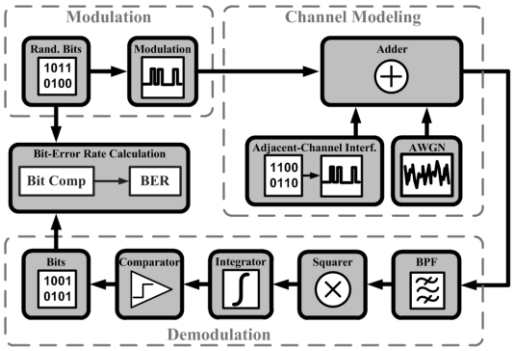

Fig 5. Block diagram of the MATLAB simulator

A. Modulation

The simulator randomly generates a stream of binary bits. These are then modulated and up-converted by the "Modulation" block using a PPM scheme with square pulses.

B. Channel Modeling

To simulate the wireless channel, additive white Gaussian noise (AWGN) and adjacent-channel interferers (ACIs) are added to the transmitted signal.

1) Noise: Since E_b/N_o is specified, then N_o can be calculated if the energy per bit, E_b, is known. The energy per bit can be calculated by squaring and integrating the modulated signal for one bit. Thus,

$$N_o = \frac{E_b}{(E_b/N_o)} = \frac{1}{SNR_{bit}} \sum_n S^2(n) \tag{21}$$

where $S(n)$ is the n^{th} sample value of the received signal, $n = 1, 2, \ldots, l$ and l is the number of samples in the transmitted signal. The one-sided noise power can be calculated as

$$P_o = \frac{N_o}{2} \cdot f_s = \frac{f_s}{2 \cdot SNR_{bit}} \sum_n S^2(n) \tag{22}$$

Then the noise signal $N(n)$ is done by generating l random values that are normally-distributed with zero-mean and standard deviation $\sigma = \sqrt{P_o}$.

2) Adjacent-Channel Interference (ACI): A To generate ACI, another random stream of bits is modulated and up-converted. The SIR value (defined as ε in section V.A) is

$$\varepsilon = \left[\sum_n S^2(n)\right] \Big/ \left[\sum_n I^2(n)\right] \tag{23}$$

where $S(n)$ is the received signal and $I(n)$ is the ACI signal. Based on (23), the pulse amplitude $|I(n)|$ for the ACI signal can be calculated using $|S(n)|$ as

$$|I(n)| = \frac{|S(n)|}{\sqrt{\varepsilon}} \tag{24}$$

where in the simulator $|S(n)| = 1$ for simplicity. Thus, $|I(n)| = 1/\sqrt{\varepsilon}$.

3) Demodulation: After the channel modeling, the demodulation part simulates the signal processing at the receiver. It filters the signal with the specified receiver bandwidth, squares it, and integrates it over periods of times

equal to T_i. Each pair of integration windows is then compared and a bit decision is made (i.e. 0 or 1)

$$\sum_n S_1^2(n) \underset{bit\ '1'}{\overset{bit\ '0'}{\gtrless}} \sum_n S_2^2(n) \qquad (25)$$

where $S_1(n)$ and $S_2(n)$ are the signals in integration window 1 and 2, respectively.

VI. Simulation Results

A. Simulation Setup validation

To validate the simulator, several simulations were run to compare the results with the known equation for BER (1). Figure 6 shows the ideal and simulated BER curves for two values of signal bandwidth and an integration time of 30 ns. The simulated values closely agree with the ideal values. Hence, the simulator can accurately predict the BER for a non-coherent PPM receiver and it will be used to corroborate the theory developed.

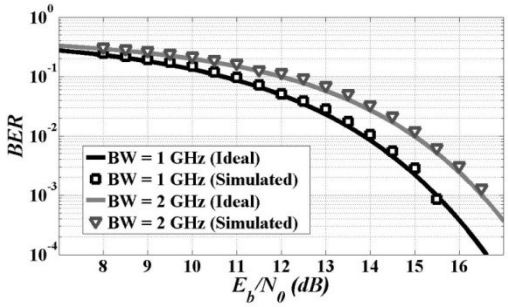

Fig 6. Bit-error rate (BER) versus SNR for two values of signal bandwidth.

B. Theory Corroboration

The main equations of this work are (8) and (18) which are expressions to calculate the BER of a non-coherent PPM receiver as a function of receiver bandwidth. Equation (8) does not consider ACI while (18) does. The other important equations are (9), (13), (19), and (20). These are just algebraic manipulations of (8) and (18). Thus, to corroborate the theory developed, it is sufficient to verify that (8) and (18) hold. Figure 7 shows a plot of BER for the ideal values obtained using (8) and the results from the simulation. It can be seen that (8) yields values that are very close to those simulated and, therefore, it holds. Similarly, figure 8 corroborate (18).

C. Analysis

Frequently, designers in wireless communications use link budgets when implementing wireless radios. An important parameter for the link budget is the E_b/N_o required to obtain a desired BER. This value can be calculated with equations (9) and (19) as a function of receiver bandwidth, desired BER and, in the case of (19), interference frequency. Figure 9 shows the required E_b/N_o as a function of the normalized receiver bandwidth to achieve a BER of 10^{-3}. Note that the lowest value of E_b/N_o corresponds to the optimal receiver bandwidth. However, a smaller receiver bandwidth can provide hardware advantages (e.g. lower sampling rate, lower power consumption) at a minimal cost in the required E_b/N_o. For instance, for a 1GHz signal, the receiver bandwidth could be reduced by half (i.e. $\beta = 0.5$) with a minimal loss in E_b/N_o of less than 1dB. If the system can tolerate this degradation, the benefits for the system will be significant (e.g. smaller sampling rate, lower power consumption, better input matching).

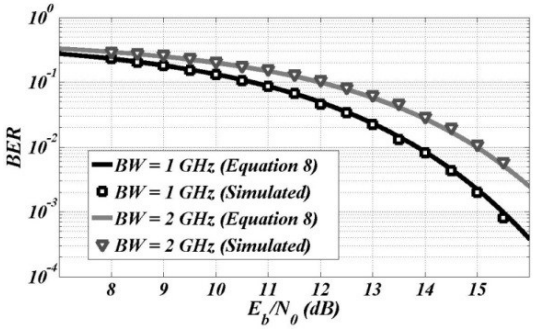

Fig 7. Bit-error rate (BER) versus SNR for two values of signal bandwidth with $\beta = 1$ (no ACI)

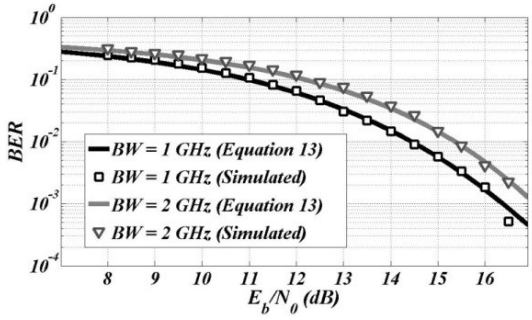

Fig 8. BER versus SNR including ACI with $\alpha = 0.8$ and $\beta = 1$

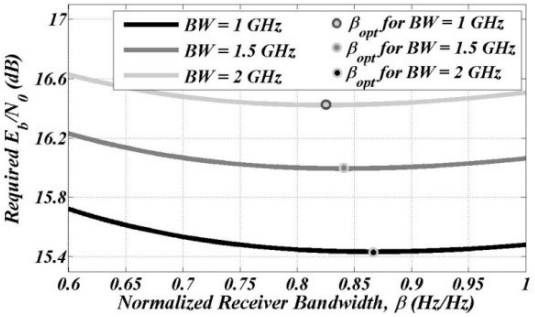

Fig 9. Required SNR_{bit} for $BER = 10^{-3}$ versus receiver bandwidth

From the same plot (figure 9), it is clear that this optimal value is a function of the signal bandwidth. Equation (13) is an accurate approximation for the optimal normalized receiver bandwidth. It is plotted in figure 10. Note that having a larger signal bandwidth increases the savings in receiver bandwidth. In other words, the optimal receiver bandwidth becomes smaller with respect to the signal bandwidth (recall $\beta = receiver\ BW/signal\ BW$) as the latter increases.

An example of the optimal receiver bandwidth when ACI is considered is also plotted in figure 10. Note that it follows a similar tendency as the curve for no ACI. However, it is shifted up. This is to be expected since the interference is effectively increasing the noise. Thus, a larger receiver bandwidth will integrate more signal energy to compensate for the added interference. However, the receiver performs worse

(i.e. required E_b/N_o increases) as the interference increases.

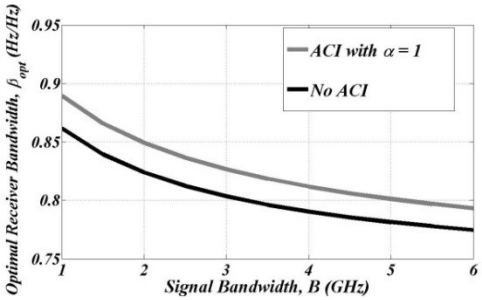

Fig 10. Normalized optimal receiver bandwidth β_{opt} versus signal bandwidth for an integration time of 30ns, a target BER of 10^{-3} and

VII. CONCLUSION

In this work, we derived equations that describe the performance of a non-coherent PPM. The theory developed here could be very useful when designing non-coherent UWB-PPM systems because it lets the designer choose easily an appropriate filter bandwidth based on the system parameters. Table III summarizes the key equations presented.

Future work will include the effect of multipath fading which causes the signal energy to be spread in time. Hence, the integration window becomes an important parameter for system performance. Smaller windows detect less signal energy and increase inter-symbol interference while larger windows integrate more noise. Therefore, there is an optimal integration time that minimizes the bit-error rate. In addition to multipath fading, alternate pulse shapes can be included in the analysis. Recalculating (7) with the equation that describes the desired pulse shape yield a new $\delta(\beta)$. This can be used to derive new equations.

TABLE III. SUMMARY OF KEY EQUATIONS

Description	Equation
Required SNR_{bit} (No ACI)	$SNR_{bit}(\beta) = \left(\frac{E_b}{N_o}\right) = \frac{K^2}{\delta(\beta)}\left(1 + \sqrt{1 + \frac{2 \cdot T_i \cdot B \cdot \beta}{K^2}}\right)$
β_{opt} (No ACI)	$\beta_{opt} \approx A_\beta + \frac{\ln(B_\beta/N)}{C_\beta + N \cdot D_\beta}$
Required SNR_{bit} (w/ ACI)	$SNR_{bit}(\alpha,\beta) = \left[\frac{\delta(\beta)}{K^2 \cdot \left(1 + \sqrt{1 + \frac{2 \cdot T_i \cdot B \cdot \beta}{K^2}}\right)} - \frac{1}{SIR_{bit}(\alpha,\beta)}\right]^{-1}$
β_{opt} (w/ ACI)	$\beta_{opt} \approx A_\beta + \frac{\ln(B_\beta/N) - (E_\beta/\alpha) \cdot \ln(F_\beta/\alpha)}{C_\beta + N \cdot D_\beta}$

REFERENCES

[1] L. Reggiani and G. M. Maggio, "Coherent vs. Non-Coherent Detection for Orthogonal Convolutional Modulation: A Trade-Off Analysis", IEEE International Conference on Ultra-Wideband, pp. 43-48, 2006.

[2] D. Chunjie, P. Orlik, Z. Sahinoglu, and A. F. Molisch, "A Non-Coherent 802.15.4a UWB Impulse Radio", IEEE International Conference on Ultra-Wideband, pp. 146-151, September 2007.

[3] F. Troesch, F. Althaus, and A. Wittneben, "Modified Pulse Repetition Coding Boosting Energy Detector Performance in Low Data Rate Systems", IEEE International Conference on Ultra-Wideband, pp. 508-513, September 2005.

[4] L. Seong-Soo, H. Sang-Min, S. Mi-Hyun, A. Dmitriev, and A. Panas, "Low Power UWB RF Transceiver for Wireless Headset", IEEE International Workshop on Radio-Frequency Integration Technology: Integrated Circuits for Wideband Communication and Wireless Sensor Networks, pp. 61-64, Novemeber 2005.

[5] F. Troesch, C. Steiner, T. Zasowski, T. Burger, and A. Wittneben, "Hardware Aware Optimization of an Ultra Low Power UWB Communication System", IEEE International Conference on Ultra-Wideband, pp 174-179, September 2007

[6] A. Rabbachin, L. Stoica, S. Tiuraniemi, and I. Oppermann, "A Low Cost, Low Power UWB Based Sensor Network", International Workshop on Wireless Ad-Hoc Networks, pp 84-88, May 2004.

[7] F. S. Lee and A. P. Chandrakasan, "A 2.5nJ/b 0.65V 3-to-5GHz Subbanded UWB Receiver in 90nm CMOS", IEEE International Solid-State Circuits Conference, pp. 116-590, February 2007.

[8] O. Klymenko, G. Fischer, and D. Martynenko, "A High Band Non-Coherent Impulse Radio UWB Receiver", IEEE International Conference on Ultra-Wideband, pp. 25-29, September 2008.

[9] A. Gerosa, M. Costa, A. Bevilacqua, D. Vogrig, and A. Neviani, "An Energy-Detector for Non-Coherent Impulse-Radio UWB Receivers", IEEE International Symp on Circuits and Systems, pp 2705-2708, 2008.

[10] M. Crepaldi, M. Casu, and M. Graziano, "Energy Detection UWB Receiver Design using a Multi-resolution VHDL-AMS Description", IEEE Workshop on Signal Processing Systems Design and Implementation, pp 13-18, Novemeber 2005.

[11] M. Yargholi and A. Nabavi, "Analog front end modules design in Non-Coherent UWB receivers for sensor networks", IEEE International Conference on Semiconductor Electronics, pp. 64-68, Novemeber 2008.

[12] S. Tiuraniemi, L. Stoica, A. Rabbachin, and I. Oppermann, "Front-End Receiver for Low Power, Low Complexity Non-coherent UWB Communications System", IEEE International Conference on Ultra-Wideband, pp 339-343, September 2005.

[13] IEEE P802.15.4a/D7, "Wireless Medium Access Control (MAC) and Physical Layer (PHY) Specifications for Low-Rate Wireless Personal Area Networks (LR-WPANs): Amendment to add alternate PHY", 2007.

[14] M. Pezzin and D. Lachartre, "A Fully Integrated LDR IR-UWB CMOS Transceiver Based on "1.5-bit" Direct Sampling", IEEE International Conference on Ultra-Wideband, pp. 642-647, September 2007

[15] Fred S. Lee and Anantha P. Chandrakasan, "A 2.5nJ/bit 0.65 V Pulsed UWB Receiver in 90 nm CMOS", IEEE Journal of Solid-State Circuits, Vol. 42, No.12, pp. 2851-2859, December 2007

[16] Marco Crepaldi, Mario R. Casu, Mariagrazia Graziano, and Maurizio Zamboni, "A Low-power CMOS 2-PPM Demodulator for Energy Detection IR-UWB Receivers", IEEE International Conference on Ultra-Wideband, pp. 461-466, September 2007

[17] J. Wu, M. Don, Q. Liang, H. Xiang, "Considaration of Pre-Filter Bandwidth Optimization for Non-Coherent UWB Receiver", IEEE International Conference on Wireless Communications, 2006.

[18] S. Dubouloz, B. Denis, S. de Rivaz, and L. Ouvry, "Performance Analysis of LDR UWB Non-Coherent Receivers in Multipath Enviroments", IEEE International Conference on Ultra-Wideband, pp. 491-496, September 2005.

[19] D. Landi and C. Fishcer, "The Effects of UWB Interference on GSM Systems", International Seminar on Communications, pp 86-89, 2004

[20] R. J. Fontana, "An Insight into UWB Interference from a Shot Noise Perspective", IEEE International Conference on Ultra-Wideband Systems and Technologies, pp318-323, 2002

[21] S.Wong and F. Lau, "Impacts of UWB Interference on Selected Radio Systems Used by the Government", IEEE International Conference on Circuits and Systems for Communications, pp 525-529, 2008

[22] J.R. Foerster, R. Schober, and L. Lampe, "Interference Modeling of Pulse-based UWB Waveforms on Narrowbands Systems", IEEE on Vehicular Technologies Conference, vol 4, pp 1931-1935, 2002

[23] A. Nasri, R. Schober and L. Lampe, "Performance of a BPSK NB Receiver in MB-ORDM UWB Interference", IEEE International Conference on Communications, vol 10, pp 4700-4705, 2006